Saturated RISE Control of Hydraulic Servo System with Modeling Uncertainties

Dongjie Bai, Zhenle Dong, Pengxiang Zhang, Zhigang Zhou, Siyuan Pan

Abstract—**The demand for high-accuracy hydraulic servo system in industry and national defense is becoming increasingly urgent. This paper focuses on the high accuracy motion tracking control of hydraulic servo system with input saturation. Firstly, nonlinear mathematical model of the valve-controlled hydraulic servo system is established, which contains the load dynamic, the pressure dynamic and the flow equation. Secondly, the state-space-equation of hydraulic servo system is constructed in integrator form to facilitate controller derivation, and a saturated controller based on RISE (robust integral of the sign of error) method is designed, which includes a model compensation term based on desired trajectory and a nonlinear RISE term in the form of hyperbolic tangent function. Then, through rigorous Lyapunov analysis, it is proven that the proposed controller can theoretically achieve asymptotic stability, while ensuring that the amplitude of control input meets the saturation limit requirements. Finally, the effectiveness of the proposed controller approach is verified through simulation of two comparative controllers under two desired trajectories with sudden disturbance.**

Index Terms—**hydraulic system; input saturation; RISE control; asymptotic stability; disturbance**

I. INTRODUCTION

DUE to its high power-to-weight ratio and strong load resistance rigidity compared with motor, the hydraulic system has been widely applied in industries and defence, such as aircraft actuation systems [1], [2], construction machinery [3], load simulators [4], etc. In recent years, the demand for hydraulic systems with high accuracy has become increasingly urgent. In this regard, the development of high-performance hydraulic components and control approaches is crucial.

Manuscript received December 30, 2024; revised April 18, 2025.

This work was supported in part by Natural Science Foundation of China under Grant 52305056, in part by Henan Province Science and Technology Research Projects under Grant 242103810050, 242102220009.

Dongjie Bai is a postgraduate student at the School of Vehicle and Transportation Engineering, Henan University of Science and Technology. Luoyang 471000, China (e-mail: b18339631260@163.com).

Zhenle Dong is an associate professor at the School of Vehicle and Transportation Engineering, Henan University of Science and Technology. Luoyang 471000, China (Corresponding author, e-mail: dong_zhenle@163.com).

Pengxiang Zhang is a postgraduate student at the School of Vehicle and Transportation Engineering, Henan University of Science and Technology. Luoyang 471000, China (e-mail: 1767858772@qq.com).

Zhigang Zhou is a Professor at the School of Vehicle and Transportation Engineering, Henan University of Science and Technology. Luoyang 471000, China (e-mail: hnmczzg@163.com).

Siyuan Pan is an assistant experimentalist at the School of Business, Henan University of Science and Technology. Luoyang 471000, China (e-mail: 499017141@qq.com).

However, hydraulic systems inherently exhibit nonlinearity and model uncertainties, which further encompass parameter uncertainties (such as friction coefficients and leakage coefficients that are prone to change with operating conditions) and disturbances (including external disturbance and difficult-to--model components, et al). These factors pose significant challenges to control design and have long been a research hotspot in hydraulic system control technology. In response, researchers have proposed numerous control methods, including adaptive robust control [5], sliding mode control [6], RISE control [7], [8], active disturbance rejection control [9], neural network control [10], fuzzy control [11], [12], among others. These methods have improved the control performance to varying degrees. Among them, RISE control, by adopting a continuous control input in integral form, can achieve asymptotic tracking in the presence of disturbances, and has been verified through applications in motor servo system [13], hydraulic servo system [7], and other scenarios.

In addition to the aforementioned control challenges, input saturation is also a frequently encountered design issue in hydraulic control systems. Input saturation refers to the phenomenon where the amplitude of control input must not exceed a certain range due to physical limitations of the system (such as restrictions on the input voltage amplitude of hydraulic valves and requirements specific to the equipment's application scenarios). However, during actual system operation, unexpected situations like mismatched initial position, external disturbance, or overloading can lead to sudden change in input signal, potentially exceeding the allowed range. When these situations occur, they inevitably compromise the effectiveness of controllers designed based on normal operating conditions, ultimately degrading the system's tracking performance. To address this issue, [14] proposes anti-windup control, which often necessitates imposing specific constraints on system signals, potentially leading to conservatism in controller design. [15] introduces model predictive control, which struggles to simultaneously handle system parameter uncertainties and disturbances, limiting their applicability to hydraulic servo systems. [16] designs an input saturation controller for linear motor servo systems, which considers both system parameter uncertainties and disturbance. However, it theoretically can only achieve bounded stability, which is not an ideal control performance. [17], focusing on Euler-Lagrange systems, realizes asymptotic stability control with input saturation by adopting the RISE method based on a hyperbolic tangent function. Nevertheless, it does not account for system parameter uncertainties.

Based on the above analysis, this paper presents a novel high-precision tracking control approach for hydraulic servo system. This approach can guarantee asymptotic tracking performance while comprehensively accounting for input saturation, disturbance, and parametric uncertainties. The RISE method is integrated to address system disturbance, and the model compensation term based on desired trajectory is devised which can be computationally efficient. Furthermore, the boundedness of the control input is achieved through employing the hyperbolic tangent function.

The subsequent content is organized as follows: Section 2 establishes the mathematical model of hydraulic servo system in integrator form to facilitate controller design, Section 3 details the derivation process of the controller, Section 4 presents rigorous control results and proofs, Section 5 contains simulation verification, and Section 6 summarizes the main conclusions.

II. Mathematical modeling

Fig. 1 shows the structure of considered hydraulic servo system. P_1, P_2 denote the oil pressure in the left and right chambers of the hydraulic cylinder; Q_1, Q_2 denote the flow rates entering and exiting the hydraulic cylinder. The servo valve controls the pressure P_1, P_2 by adjusting the flow rate Q_1, Q_2, thereby controlling the extension length y of the piston rod, which is connected to the inertia load.

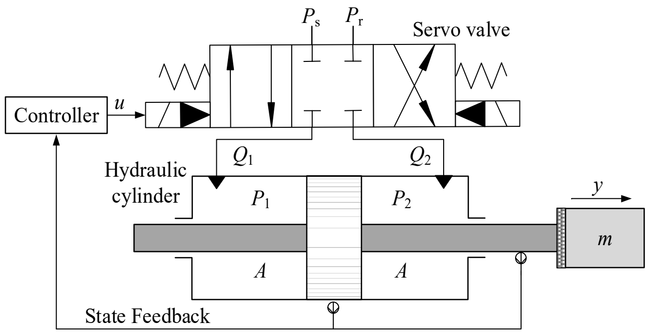

Fig. 1. Structure of considered hydraulic servo system

The dynamic of the inertia load is

$$m\ddot{y} = P_{\mathrm{L}}A - B\dot{y} - f(t) \tag{1}$$

where m is the mass of the inertial load; y, $\dot{y}$ and $\ddot{y}$ denotes displacement, velocity and acceleration of the inertial load respectively; $P_{\mathrm{L}}=P_1-P_2$ is the load pressure; A is the ram area of the chamber; B is the viscous friction parameter; $f(t)$ denotes the unstructured uncertainty which contains unmodeled friction, external disturbance and other hard-to-model terms.

Neglecting the external leakage, the load pressure dynamic in the actuators can be written as

$$\frac{V_{\mathrm{t}}}{4\beta_{\mathrm{e}}}\dot{P}_{\mathrm{L}} = Q_{\mathrm{L}} - A\dot{y} - C_{\mathrm{t}}P_{\mathrm{L}} + Q_{\mathrm{d}} \tag{2}$$

where Vt denotes the total control volume; β_{e} denotes the effective bulk modulus; Q_{L} denotes the load flow; C_{t} denotes the internal leakage coefficient of the cylinder; Q_{d} denotes the modelling error.

Q_{L} can be modelled as

$$Q_{\mathrm{L}} = k_{\mathrm{v}}x_{\mathrm{v}} - k_{\mathrm{c}}P_{\mathrm{L}} \tag{3}$$

where k_{v} is the flow gain with respect to the valve core displacement x_{v}; k_{c} is the gain with respect to load pressure. Considering that high response servo valve is used, we can neglect the servo valve dynamic as in [18], i.e., $x_{\mathrm{v}} = k_{\mathrm{u}}u$.

The control objective can be summarized as: given the desired trajectory $x_{1\mathrm{d}}$, then to derive a control input u such that the actual output x_1 tracks $x_{1\mathrm{d}}$ as closely as possible, while to ensure that the amplitude of u meets saturation limit, i.e.,

$$|u| \le u_{\mathrm{sat}} \tag{4}$$

where u_{sat} denotes a known saturation limit.

III. Controller design

Define the state variables $x = [x_1, x_2, x_3]^{\mathrm{T}} = [y, \dot{y}, \ddot{y}]^{\mathrm{T}}$, then the entire system can be expressed in a state-space form as

$$\begin{aligned} \dot{x}_1 &= \dot{x}_2 \\ \dot{x}_2 &= \dot{x}_3 \\ \theta_1\dot{x}_3 &= u - \theta_2 x_2 - \theta_3 x_3 + \delta(t) \end{aligned} \tag{5}$$

where

$$\theta_1 = \frac{mV_{\mathrm{t}}}{4Ak_{\mathrm{g}}\beta_{\mathrm{e}}}, \quad \theta_2 = \frac{A}{k_{\mathrm{g}}} + \frac{k_{\mathrm{t}}B}{Ak_{\mathrm{g}}}$$

$$\theta_3 = \frac{k_{\mathrm{t}}m}{Ak_{\mathrm{g}}} + \frac{BV_{\mathrm{t}}}{4Ak_{\mathrm{g}}\beta_{\mathrm{e}}}$$

$$\delta(t) = \frac{Q_{\mathrm{d}}}{k_{\mathrm{g}}} - \frac{k_{\mathrm{t}}f(t)}{Ak_{\mathrm{g}}} + \frac{V_{\mathrm{t}}\dot{f}(t)}{4Ak_{\mathrm{g}}\beta_{\mathrm{e}}}$$

$$k_{\mathrm{t}} = k_{\mathrm{c}} + C_{\mathrm{t}}, \quad k_{\mathrm{g}} = k_{\mathrm{v}}k_{\mathrm{u}}$$

Assumption 1: In general working conditions, according to the definition of P_1 and P_2, the system states of hydraulic system, P_1 and P_2 are both bounded, i.e., $0 < P_{\mathrm{r}} < P_1 < P_{\mathrm{s}}$, $0 < P_{\mathrm{r}} < P_2 < P_{\mathrm{s}}$, where P_{s}, P_{r} denotes the pressure of supplied oil and returned oil.

Assumption 2: Although the true value of the parameter set $\theta = [\theta_1, \theta_2, \theta_3]^{\mathrm{T}}$ is unknown, the range of the parameter uncertainties is known for most applications, i.e.,

$$\theta \in \Omega_\theta = \{\theta : \theta_{in} \le \theta \le \theta_{\max}\} \tag{6}$$

where $\theta_{\min} = [\theta_{1\min}, \ldots, \theta_{3\min}]^{\mathrm{T}}$, $\theta_{\max} = [\theta_{1\max}, \ldots, \theta_{3\max}]^{\mathrm{T}}$.

To facilitate the controller design, the nominal value will be adopted for system parameters, and then model (5) can be transformed to:

$$\begin{aligned} \dot{x}_1 &= \dot{x}_2 \\ \dot{x}_2 &= \dot{x}_3 \\ \theta_{1\mathrm{n}}\dot{x}_3 &= u - \theta_{2\mathrm{n}}x_2 - \theta_{3\mathrm{n}}x_3 + \Delta(t) \end{aligned} \tag{7}$$

where

$$\Delta(t) = \delta(t) - (\theta_1\dot{x}_3 - \theta_{1\mathrm{n}}\dot{x}_3) - (\theta_2 x_2 - \theta_{2\mathrm{n}}x_2) - (\theta_3 x_3 - \theta_{3\mathrm{n}}x_3)$$

Assumption 3: The first-order and second-order derivative of total disturbance $\Delta(t)$ are bounded, i.e.,

$$|\dot{\Delta}(t)| \le \sigma_1, \quad |\ddot{\Delta}(t)| \le \sigma_2 \tag{8}$$

where σ_1, σ_2 are known constants.

Remake 1: According to formula (1)(2)(5)(7), it is evident that the total disturbance $\Delta(t)$ is mainly related to $f(t)$, Q_{d}, and system parameters. For $f(t)$, its main component is unmodeled friction of hydraulic system. Since it is impossible for hydraulic system to generate discontinuous force during operation, the friction can be considered continuous. For Q_{d}, its main component is the external leakage of hydraulic cylinder, which can also be regarded as continuous. Additionally, although the system parameters are unknown, they always change slowly and the system states are also continuously varying. It is therefore straightforward to deduce that the total disturbance in the system is always bounded, smooth, and continuous, which validates the rationality of Assumption 3.

Define the tracking error as $z_1 = x_1 - x_{1d}$. In addition, define a set of quantities as

$$
\begin{aligned}
z_2 &= \dot{z}_1 + k_1 z_1, \\
z_3 &= \dot{z}_2 + k_2 z_2 + \tanh(z_f) \\
\dot{z}_f &= \cosh^2(z_f)[-\gamma_1 k_{r1} z_3 - k_{r2}\tanh(z_f)] \\
r &= \dot{z}_3 + k_3 z_3
\end{aligned} \tag{9}
$$

where k_1, k_2, k_3, k_{r1}, k_{r2}, γ_1 are positive feedback gains, $r(t)$ is an auxiliary error signal to get an extra design freedom. It is easy to check that the filtered error $r(t)$ could not be measured because it depends on the time derivative of acceleration signal, in fact, its main function is just to help the following controller design and will not appear in the final controller.

From (9), r can be expressed as

$$
\begin{aligned}
r &= \dot{x}_3 - \dddot{x}_{1d} + (k_1 + k_2 + k_3 - \gamma_1 k_{r1}) z_3 \\
&\quad -(k_1 k_2 + k_1^2 + k_2^2) z_2 + k_1^3 z_1 - (k_1 + k_2 + k_{r2})\tanh(z_f)
\end{aligned} \tag{10}
$$

Based on formula (7) and (10), we can arrive at

$$
\begin{aligned}
\theta_{1n} r &= u - \theta_{1n}\dddot{x}_{1d} - \theta_{2n} x_2 - \theta_{3n} x_3 + \Delta(t) \\
&\quad + \theta_{1n}(k_1 + k_2 + k_3 - \gamma_1 k_{r1}) z_3 \\
&\quad - \theta_{1n}(k_1 k_2 + k_1^2 + k_2^2) z_2 + \theta_{1n} k_1^3 z_1 \\
&\quad - \theta_{1n}(k_1 + k_2 + k_{r2})\tanh(z_f) \\
&= u - \theta_{1n}\dddot{x}_{1d} - \theta_{2n}\dot{x}_{1d} - \theta_{3n}\ddot{x}_{1d} + \Delta(t) \\
&\quad + [\theta_{1n}(k_1 + k_2 + k_3 - \gamma_1 k_{r1}) - \theta_{3n}] z_3 \\
&\quad - [\theta_{1n}(k_1 k_2 + k_1^2 + k_2^2) + \theta_{2n} - \theta_{3n}(k_1 + k_2)] z_2 \\
&\quad + (\theta_{1n} k_1^3 + \theta_{2n} k_1 - \theta_{3n} k_1^2) z_1 \\
&\quad - [\theta_{1n}(k_1 + k_2 + k_{r2}) + \theta_{3n}]\tanh(z_f)
\end{aligned} \tag{11}
$$

Then the final controller can be designed as

$$
\begin{aligned}
u &= u_a + u_s \\
u_a &= \theta_{1n}\dddot{x}_{1d} + \theta_{2n}\dot{x}_{1d} + \theta_{3n}\ddot{x}_{1d} \\
u_s &= \gamma_1 \tanh(v) \\
\dot{v} &= \cosh^2(v)[-k_{r1} k_3 z_3 - \beta\,\mathrm{sign}(z_3)]
\end{aligned} \tag{12}
$$

where u_a is a mode-based compensation term based on desired trajectory, u_s is a nonlinear robust control term to cope with the total disturbance $\Delta(t)$, γ_1 and β are positive feedback gains.

Further from the expression of control input, we know

$$
u \le \theta_{1n}|\dddot{x}_{1d}| + \theta_{2n}|\dot{x}_{1d}| + \theta_{3n}|\ddot{x}_{1d}| + \gamma_1 = \bar{u} \tag{13}
$$

To satisfy inequality (4), it is sufficient to select $\bar{u}$ appropriately such that it is less than u_{sat}.

The controller design is completed. Structure of the proposed controller is shown in Fig. 2.

IV. Main Results

Substituting (12) into (11), we can obtain

$$
\begin{aligned}
\theta_{1n} r &= u_s + \Delta(t) + [\theta_{1n}(k_1 + k_2 + k_3 - \gamma_1 k_{r1}) - \theta_{3n}] z_3 \\
&\quad - [\theta_{1n}(k_1 k_2 + k_1^2 + k_2^2) + \theta_{2n} - \theta_{3n}(k_1 + k_2)] z_2 \\
&\quad + (\theta_{1n} k_1^3 + \theta_{2n} k_1 - \theta_{3n} k_1^2) z_1 \\
&\quad - [\theta_{1n}(k_1 + k_2 + k_{r2}) + \theta_{3n}]\tanh(z_f)
\end{aligned} \tag{14}
$$

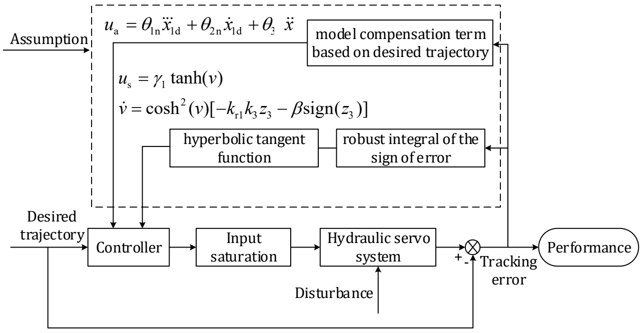

Fig. 2. Structure of the proposed controller

then the time derivative of (14) can be given by

$$
\begin{aligned}
\theta_{1n}\dot{r} &= -\gamma_1 k_{r1} k_3 z_3 - \gamma_1\beta\,\mathrm{sign}(z_3) + \dot{\Delta}(t) - \gamma_1 k_{r1}\dot{z}_3 \\
&\quad + [\theta_{1n}(k_1 + k_2 + k_3) - (\theta_{1n} - 1)\gamma_1 k_{r1} - \theta_{3n}]\dot{z}_3 \\
&\quad - [\theta_{1n}(k_1 k_2 + k_1^2 + k_2^2) + \theta_{2n} - \theta_{3n}(k_1 + k_2)]\dot{z}_2 \\
&\quad + (\theta_{1n} k_1^3 + \theta_{2n} k_1 - \theta_{3n} k_1^2)\dot{z}_1 \\
&\quad - [\theta_{1n}(k_1 + k_2 + k_{r2}) + \theta_{3n}]\dot{\tanh}(z_f) \\
&= -\gamma_1 k_{r1} r - \gamma_1\beta\,\mathrm{sign}(z_3) + \dot{\Delta}(t) \\
&\quad + c_1 r + c_2 z_3 + c_3 z_2 + c_4 z_1 + c_5\tanh(z_f)
\end{aligned} \tag{15}
$$

where

$$
\begin{aligned}
c_1 &= \theta_{1n}(k_1 + k_2 + k_3) - (\theta_{1n} - 1)\gamma_1 k_{r1} - \theta_{3n} \\
c_2 &= [\theta_{1n}(k_1 + k_2 + k_3 + k_{r2}) + \theta_{3n} + k_3]\gamma_1 k_{r1} \\
&\quad - \theta_{1n}(k_1 k_3 + k_2 k_3 + k_3^2 + k_1 k_2 + k_1^2 + k_2^2) \\
&\quad - \theta_{2n} + \theta_{3n}(k_1 + k_2 + k_3) \\
c_3 &= \theta_{1n}(k_1 k_2^2 + k_1^2 k_2 + k_2^3 + k_1^3) + \theta_{2n}(k_1 + k_2) \\
&\quad - \theta_{3n}(k_1^2 + k_1 k_2 + k_2^2) \\
c_4 &= \theta_{3n} k_1^3 - \theta_{1n} k_1^4 - \theta_{2n} k_1^2 \\
c_5 &= \theta_{1n}(k_1 k_2 + k_1^2 + k_2^2 + k_1 k_{r2} + k_2 k_{r2} + k_{r2}^2) + \theta_{2n} \\
&\quad - \theta_{3n}(k_1 + k_2 + k_{r2})
\end{aligned}
$$

Lemma 1: An auxiliary function $P(t)$ is defined as

$$
P(t) = r[\dot{\Delta}(t) - \gamma_1\beta\,\mathrm{sign}(z_3)] \tag{16}
$$

Provided that the feedback gain β is chosen to satisfy

$$
\beta \ge \frac{\delta_1 + \delta_2 / k_3}{\gamma_1} \tag{17}
$$

thus, the function $H(t)$ defined below is always non-negative [19]

$$
H(t) = \beta|z_3(0)| - z_3(0)\dot{\Delta}(t) - \int_0^t P(\kappa)d\kappa \tag{18}
$$

Proof of Lemma 1:

From (16) and (18), we have

$$
\begin{aligned}
\int_0^t P(\kappa)d\kappa &= \int_0^t (\dot{z}_3 + k_3 z_3)[\dot{\Delta}(t) - \gamma_1\beta\,\mathrm{sign}(z_3)]d\kappa \\
&= \int_0^t \dot{z}_3\dot{\Delta}(t)d\kappa - \int_0^t z_3\gamma_1\beta\,\mathrm{sign}(z_3)]d\kappa \\
&\quad + \int_0^t k_3 z_3[\dot{\Delta}(t) - \gamma_1\beta\,\mathrm{sign}(z_3)]d\kappa \\
&= z_3\dot{\Delta}(t)\Big|_0^t - \int_0^t z_3\ddot{\Delta}(t)d\tau - \gamma_1\beta|z_3(0)|\Big|_0^t \\
&\quad + \int_0^t k_3 z_3[\dot{\Delta}(t) - \gamma_1\beta\,\mathrm{sign}(z_3)]d\kappa \\
&= z_3\dot{\Delta}(t) - z_3(0)\dot{\Delta}(0)| - \gamma_1\beta|z_3| + \gamma_1\beta|z_3(0)| \\
&\quad + \int_0^t k_3|z_3|[|\dot{\Delta}(t)| - \frac{1}{k_3}|\ddot{\Delta}(t)| - \gamma_1\beta]d\kappa
\end{aligned} \tag{19}
$$

Obviously from (6) and (19), the function $H(t)$ defined in (18) is always non-negative provided that inequality (17) is satisfied. This completes the proof.

Theorem 1: By choosing feedback gains k_1, k_2, k_3, k_{r1} and k_{r2} large enough, the following defined matrix Λ can be positive definite

$$\Lambda=\begin{bmatrix} k_1 & -\frac{1}{2} & 0 & 0 & -\frac{c_4}{2} \\ -\frac{1}{2} & k_2 & -\frac{1}{2} & \frac{1}{2} & -\frac{c_3}{2} \\ 0 & -\frac{1}{2} & k_3 & \frac{\gamma_1 k_{r1}}{2} & -\frac{c_2+1}{2} \\ 0 & -\frac{1}{2} & \frac{\gamma_1 k_{r1}}{2} & k_{r2} & -\frac{c_5}{2} \\ -\frac{c_4}{2} & -\frac{c_3}{2} & -\frac{c_2+1}{2} & -\frac{c_5}{2} & \sigma \end{bmatrix} \quad (20)$$

where $\sigma=\gamma_1 k_{r1}-c_1$, then the proposed controller (12) can guarantee that all signals in the closed-loop system are bounded, and asymptotic tracking can also be achieved, i.e., $z_1 \rightarrow 0$ as $t \rightarrow \infty$.

Proof of Theorem 1:

Define the following Lyapunov function:

$$V=\frac{1}{2}z_1^2+\frac{1}{2}z_2^2+\frac{1}{2}z_3^2+\frac{1}{2}\theta_{1n}r^2+\frac{1}{2}\tanh^2(z_f)+H \quad (21)$$

Taking the derivative of V, we have

$$\begin{aligned} \dot{V} &= \frac{1}{2}z_1^2+\frac{1}{2}z_2^2+\frac{1}{2}z_3^2+\frac{1}{2}\theta_{1n}r^2+\frac{1}{2}\tanh^2(z_f)+H \\ &= z_1\dot{z}_1+z_2\dot{z}_2+z_3\dot{z}_3+r\theta_{1n}\dot{r}+\tanh(z_f)\dot{\tanh}(z_f)+\dot{H} \\ &= z_1(z_2-k_1z_1)+z_2[z_3-k_2z_2-\tanh(z_f)]+z_3(r-k_3z_3) \\ &\quad +r[-\gamma_1k_{r1}r-\gamma_1\beta\text{sign}(z_3)+\dot{\Delta}(t)+c_1r+c_2z_3+c_3z_2 \\ &\quad +c_4z_1+c_5\tanh(z_f)] \\ &\quad +\tanh(z_f)[-\gamma_1k_{r1}z_3-k_{r2}\tanh(z_f)]-P \\ &= -k_1z_1^2-k_2z_1^2-k_3z_1^2-k_{r2}\tanh^2(z_f)-\sigma r^2+z_1z_2 \\ &\quad +c_4z_1r+z_2z_3-z_2\tanh(z_f)+c_3z_2r-\gamma_1k_{r1}z_3\tanh(z_f) \\ &\quad +(c_2+1)z_3r+c_5\tanh(z_f)r \\ &= -z^{T}\Lambda z \end{aligned} \quad (22)$$

Then, as long as matrix Λ is positive definite, the following inequality holds

$$\dot{V}\le-\lambda_{\min}(\Lambda)[z_1^2+z_1^2+z_1^2+\tanh^2(z_f)]=-W \quad (23)$$

where $\lambda_{\min}(\Lambda)$ denotes the minimum eigenvalue of matrix Λ. By analyzing formula (21)-(23), it can be concluded that Lyapunov function V is bounded, and consequently $W \in L_2$, and further, tracking error z_1 and z_2, z_3, $\tanh(z_f)$, r are also bounded. Combining with formula (9)(12), it can be deduced that all signals in the closed-loop system are bounded, and thus W is bounded. Based on Barbalat's Lemma [20], W is uniformly continuous, which means that as $t \rightarrow \infty$, $W \rightarrow 0$, i.e., $z_1 \rightarrow 0$, thereby asymptotic tracking can be achieved for hydraulic servo system in the presence of input saturation. This completes the proof.

Remake 2: Some advantages of the designed controller are as follows: (i) The state-related quantities in the controller are replaced by the desired trajectory and its derivatives, which effectively mitigating the impact of measurement noise on states. (ii) The adoption of the desired trajectory and its derivatives can also significantly reduce the online calculation time of control input. (iii) The control input is continuous, making it practical for actual hydraulic systems. (iiii) The upper bound of control input can be adjusted through parameter γ_1, which ensures that the proposed controller can be applied to various input saturation situations.

V. Verification

Simulation verification is carried out based on the system shown in Fig. 1, MATLAB/Simulink is selected as simulation platform, and S-function module is used to calculate the control input.

Specifications of the considered hydraulic servo system are as follows:

TABLE I
SPECIFICATIONS OF THE CONSIDERED HYDRAULIC SERVO SYSTEM

Symbol	Value	Symbol	Value
m	30kg	β_e	700MPa
B	4000$N\cdot s/m$	k_g	1.18×10^{-8} $m^4/(s\cdot V\cdot N^{-1/2})$
A	$9\times10^{-4}m^2$	k_t	9×10^{-12} $m^5/(N\cdot s)$
V_t	$7.96\times10^{-5}m^3$		

To fully verify the effectiveness, the following two controllers are selected for comparison:

(1) SRISE: the detailed structure has been given in (12). By trial-and-error, the control parameters are chosen as: k_1 = 50, k_2 = 100, k_3 = 50, k_{r1} = 20, k_{r2} = 10, β = 0.05.

(2) RISE: this is the RISE control proposed in [21], which does not consider the effect from input saturation. By referring to [21], the detailed structure of RISE controller is:

$$\begin{aligned} & z_2=\dot{z}_1+k_1z_1,\quad z_3=\dot{z}_2+k_2z_2,\quad r=\dot{z}_3+k_3z_3 \\ & u=u_a+u_s \\ & u_a=\theta_{1n}\dddot{x}_{1d}+\theta_{2n}\dot{x}_{1d}+\theta_{3n}\ddot{x}_{1d} \\ & u_s=-k_{r1}z_3-\int_0^t k_{r1}k_3z_3+\beta\text{sign}(z_3)dv \end{aligned} \quad (24)$$

To ensure that the comparison is valid, the controller parameters are taken to be the same as the corresponding parameters of SRISE, i.e., k_1 = 50, k_2 = 100, k_3 = 50, k_{r1} = 20, β = 0.05.

Case 1：

A smooth sine-like trajectory x_{1d} = 20sin(πt)(1-exp(-0.01 t^3))mm shown in Fig. 3 is chosen as the desired trajectory. The simulation time is 0-20s, with a sampling interval 0.0002s. A sinusoidal disturbance with an amplitude of 1000N is added at 10-12s, as shown in Fig. 4. The saturation limit of control input is set as u_{sat} =0.8V, and γ_1 = 0.7. The simulation results are shown in Fig. 5-6.

As can be seen from Fig. 5, thanks to the hyperbolic tangent function, control input of the proposed SRISE controller remains within the saturation limit at all times, whereas control input of RISE controller reaches the saturation limit when faced with disturbance, specifically at 12-12.5s. According to Fig. 6, tracking error of the proposed SRISE controller is significantly smaller than that of RISE controller. Moreover, when faced with disturbance, tracking error of the proposed SRISE controller exhibits no fluctuations, whereas RISE controller experiences notable error fluctuations at 10-12s.

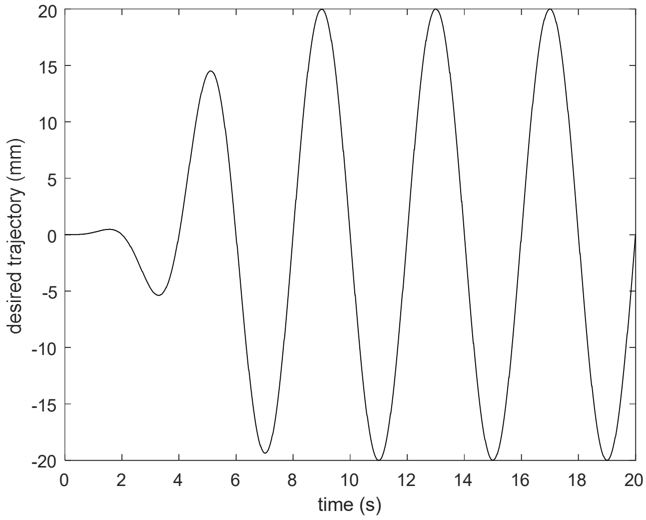

Fig. 3. The desired trajectory

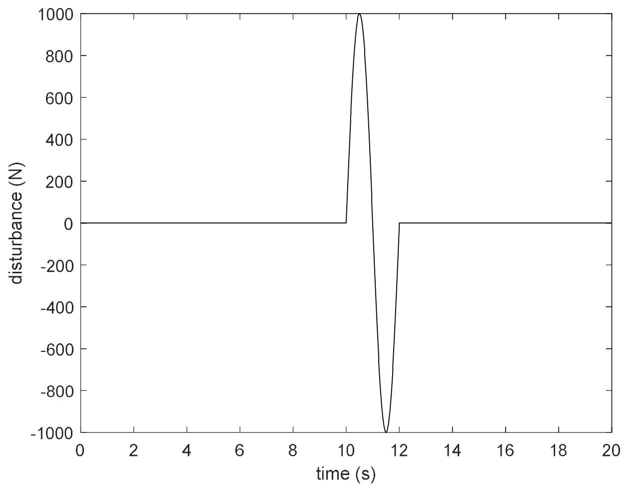

Fig. 4. Disturbance

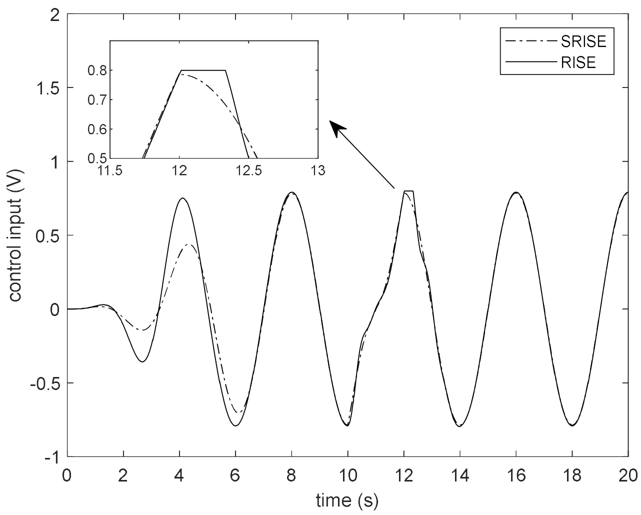

Fig. 5. Control input

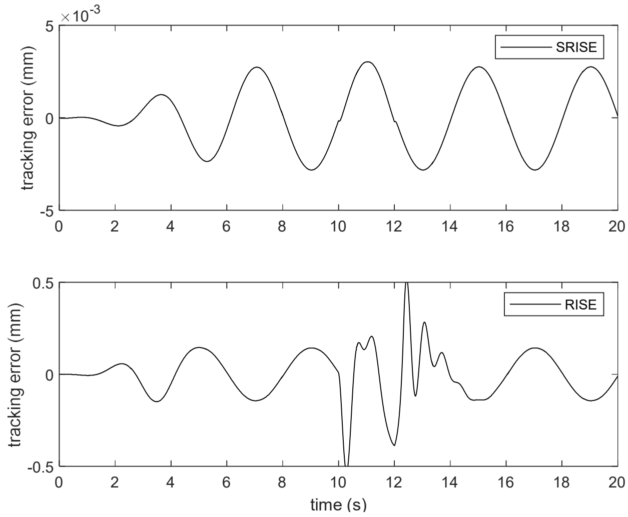

Fig. 6. Tracking error

Case 2:

A point-to-point trajectory with the amplitude of 20mm shown in Fig. 7 is chosen as the desired trajectory. The simulation time is 0-20s, with a sampling interval 0.0002s. A sinusoidal disturbance as in case 1 is added. The saturation limit of control input is set as u_{sat} =0.6V, and γ_1 = 0.6. The simulation results are shown in Fig. 8-9.

As can be seen from Fig. 8, thanks to the hyperbolic tangent function, control input of the proposed SRISE controller remains within the saturation limit at all times, whereas control input of RISE controller reaches the saturation limit when faced with disturbance, specifically at 10.5-11s. According to Fig. 9, tracking error of the proposed SRISE controller is significantly smaller than that of RISE controller. Moreover, when faced with disturbance, tracking error of the proposed SRISE controller exhibits no fluctuations, whereas RISE controller experiences notable error fluctuations at 10-12s.

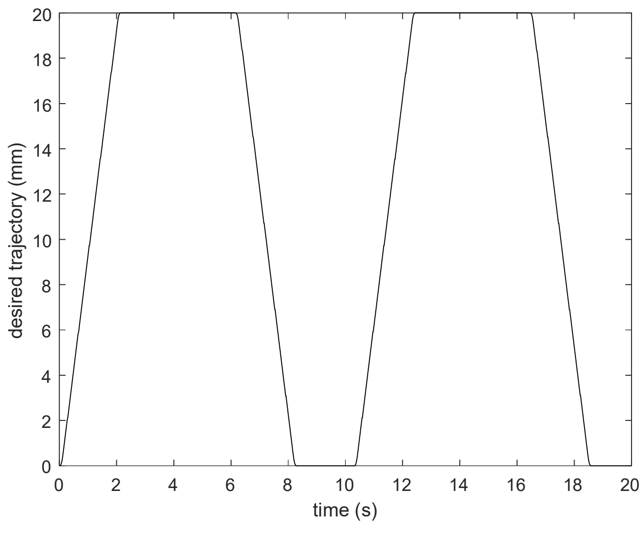

Fig. 7. The desired trajectory

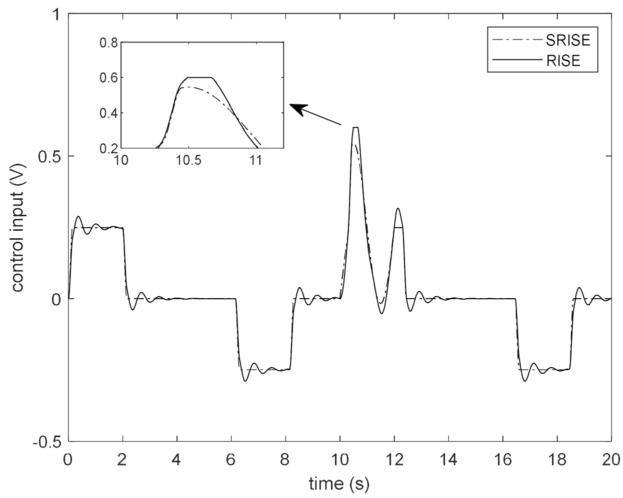

Fig. 8. Control input

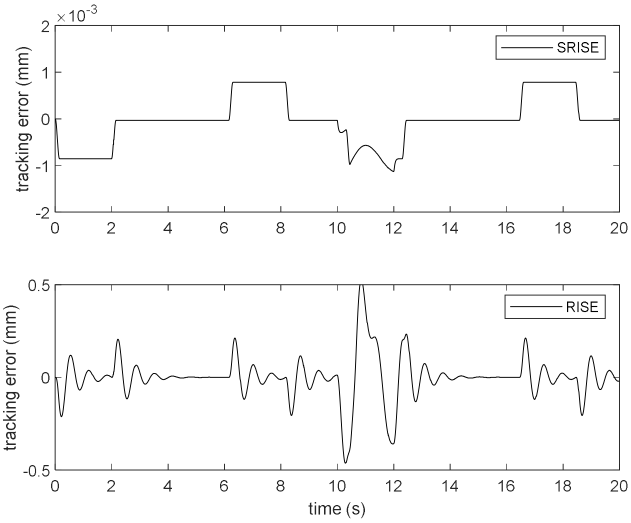

Fig. 9. Tracking error

VI. CONCLUSION

This paper proposes a saturated RISE control approach for hydraulic servo systems with input saturation, and the theoretical performance is analyzed based on the rigorous Lyapunov method. Through comparative simulations of tracking performance with the traditional RISE method under two desired trajectories, it is verified that the proposed controller can significantly improve control accuracy while ensuring the control input remains within the saturation limit. The approach proposed in this paper can be extended to various application scenarios of hydraulic servo systems with input saturation. Future research will focus on the efficient tuning methods of controller parameters.

REFERENCES

[1] Z. Jiao, N. Bai, X. Liu, J. Li, Z. Wang, D. Sun, P. Qi, and Y. Shang, "Aircraft Anti-skid Braking Control Technology: A Review," *Acta Aeronautica et Astronautica Sinica,* vol. 43, no. 10, pp. 442-446, 2022.

[2] Zhanlong Li, Haotian Hou, Zheng Zhang, Beijun Guo, Yong Song, and Zhiqi Liu, "Analysis of Vehicle Ride Comfort and Parameter Optimization of Hydro-pneumatic Suspension for Heavy Duty Mining Vehicle," Engineering Letters, vol. 32, no. 11, pp2145-2152, 2024.

[3] F. Zhang, J. Zhang, M. Cheng, and B. Xu, "A Flow-Limited Rate Control Scheme for the Master-Slave Hydraulic Manipulator," *IEEE Transactions on Industrial Electronics,* vol. 69, no. 5, pp. 4988-4998, 2022.

[4] J. Yao, Z. Jiao, and D. Ma, "High Dynamic Adaptive Robust Control of Load Emulator with Output Feedback Signal," *Journal of the Franklin Institute,* vol. 351, no. 8, pp. 4415-4433, 2014.

[5] Z. Dong, D. Ma, Q. Liu, and X. Yue, "Motion Control of Valve-controlled Hydraulic Actuators with Input Saturation and Modelling Uncertainties," *Advances in Mechanical Engineering,* vol. 10, no. 11, pp. 1-8, 2018.

[6] Z. Dong, and J. Ma, "Quasi-Adaptive Sliding Mode Motion Control of Hydraulic Servo-Mechanism with Modeling Uncertainty: A Barrier Function-Based Method," *IEEE Access,* vol. 8, pp. 143359-143365, 2020.

[7] Z. Yao, J. Yao, and W. Sun, "Adaptive RISE Control of Hydraulic Systems with Multilayer Neural-Networks," *IEEE Transactions on Industrial Electronics,* vol. 66, no. 11, pp. 8638-8647, 2019.

[8] Yinghao Yang, Zhenle Dong, Zhigang Zhou, Zheng Zhang, Geqiang Li, and Yugong Dang, "RISE based Synchronous Control of Dual Electro-hydraulic Servo System via Internal Force Adjustment," Engineering Letters, vol. 30, no.3, pp1146-1151, 2022.

[9] J. Yao, and W. Deng, "Active Disturbance Rejection Adaptive Control of Hydraulic Servo Systems," *IEEE Transactions on Industrial Electronics,* vol. 64, no. 10, pp. 8023-8032, 2017.

[10] G. Yang, J. Yao, and Z. Dong, "Neuroadaptive Learning Algorithm for Constrained Nonlinear Systems with Disturbance Rejection," *International Journal of Robust and Nonlinear Control,* vol. 32, no. 10, pp. 6127-6147, 2022.

[11] Y. Wang, Y. Zhao, M. Liang, and K. Zhang, "Embedded Navigation system of Mechatronics Robot by Fuzzy Control," International Journal of Mechatronics and Applied Mechanics, " vol. 14, pp. 128-136, 2023.

[12] Yuan Wei, Haoran Li, Zhigang Zhou, and Dongdong Chen, "Driving Path Tracking Strategy of Humanoid Robot Based on Improved Pure Tracking Algorithm," IAENG International Journal of Applied Mathematics, vol. 54, no. 2, pp286-297, 2024.

[13] Z. Dong, J. Yao, and D. Ma, "Asymptotic Tracking Control of Motor Servo System with Input Constraint," *Acta Armamentarii,* vol. 36, no. 8, pp. 1405-1410, 2015.

[14] D. Dai, T. Hu, A. R. Teel, and L. Zaccarian, "Output Feedback Design for Saturated Linear Plants Using Deadzone Loops," *Automatica,* vol. 45, no. 12, pp. 2917-2924, 2009.

[15] F. Cuzzla, J. Geromel, and M. Morari, "An Improved Approach for Constrained Robust Model Predictive Control,". *Automatica,* vol. 38, no. 7, pp. 1183-1189, 2002.

[16] S. Gayaka, L. Lu, and B. Yao, "Global Stabilization of a Chain of Integrators with Input Saturation and Disturbances: A New Approach," *Automatica,* vol. 48, no. 7, pp. 1389-1396, 2012.

[17] N. Fischer, Z. Kan, R. Kamalapurkar, and W. E. Dixon, "Saturated RISE Feedback Control for a Class of Second-Order Nonlinear Systems," *IEEE Transactions on Automatic Control,* vol. 59, no. 4, pp. 1094-1099, 2014.

[18] J. Yao, Z. Jiao, and D. Ma, "Extended-State-Observer-Based Output Feedback Nonlinear Robust Control of Hydraulic Systems with Backstepping," *IEEE Transactions on Industrial Electronics,* vol. 61, no. 11, pp. 6285-6293, 2014.

[19] B. Xian, D.M. Dawson, M.S.de Queiroz, and J. Chen, "A Continuous Asymptotic Tracking Control Strategy for Uncertain Nonlinear Systems," *IEEE Transactions on Automatic Control,* vol. 49, no. 7, pp. 1206-1211, 2004.

[20] M. Krstic, I. Kanellakopoulos, and P.V. Kokotovic, "Nonlinear and Adaptive Control Design," New York: Wiley, 1995.

[21] J. Yao, W. Deng, and Z. Jiao, "RISE-Based Adaptive Control of Hydraulic Systems with Asymptotic Tracking," *IEEE Transactions on Automation Science and Engineering,* vol. 14, no. 3, pp. 1524-1531, 2015.